

Initialization of Single Spin Dressed States using Shortcuts to Adiabaticity

J. Kölbl,¹ A. Barfuss,¹ M. S. Kasperczyk,¹ L. Thiel,¹ A. A. Clerk,² H. Ribeiro,³ and P. Maletinsky^{1,*}

¹*Department of Physics, University of Basel, Basel 4056, Switzerland*

²*Institute for Molecular Engineering, University of Chicago, Chicago, Illinois 60637, USA*

³*Max Planck Institute for the Science of Light, Erlangen 91058, Germany*



(Received 11 December 2018; published 5 March 2019)

We demonstrate the use of shortcuts to adiabaticity protocols for initialization, read-out, and coherent control of dressed states generated by closed-contour, coherent driving of a single spin. Such dressed states have recently been shown to exhibit efficient coherence protection, beyond what their two-level counterparts can offer. Our state transfer protocols yield a transfer fidelity of $\sim 99.4(2)\%$ while accelerating the transfer speed by a factor of 2.6 compared to the adiabatic approach. We show bidirectionality of the accelerated state transfer, which we employ for direct dressed state population read-out after coherent manipulation in the dressed state manifold. Our results enable direct and efficient access to coherence-protected dressed states of individual spins and thereby offer attractive avenues for applications in quantum information processing or quantum sensing.

DOI: [10.1103/PhysRevLett.122.090502](https://doi.org/10.1103/PhysRevLett.122.090502)

The pursuit of protocols for quantum sensing [1,2] and quantum information processing [3,4] builds on established techniques for initializing, coherently manipulating, and reading out quantum states, as extensively demonstrated in, e.g., trapped ions [5,6], solid-state qubits [7], and color center spins [8]. Importantly, the involved quantum states need to be protected from decoherence [9], which is primarily achieved by pulsed dynamical decoupling [10–12], a technique that suffers from drawbacks including experimental complexity and vulnerability to pulse errors. In contrast, dressed states generated by continuous driving of a quantum system yield efficient coherence protection [13–16], even for comparatively weak driving fields [17], in a robust, experimentally accessible way that is readily combined with quantum gates [18–20].

A major bottleneck for further applications of such dressed states, however, is the difficulty in performing fast, high-fidelity initialization into individual, well-defined dressed states. Up to now, such initialization has focused on two-level systems and has mainly used adiabatic state transfer [18,19], without detailed characterization of the resulting fidelities. Adiabatic state transfer, however, suffers from a tradeoff between speed and fidelity: The initialization must be slow to maintain fidelity, but fast enough to avoid decoherence during state transfer. For experimentally achievable driving field strengths, this tradeoff and the remaining sources of decoherence form a key limitation to further advances in the use of dressed states in quantum information processing and sensing.

Here, we overcome these limitations with a twofold approach, where we employ recently developed protocols for “shortcuts to adiabaticity” (STA) [21–25] and apply them to the initialization of three-level dressed states that

exhibit efficient coherence protection, beyond what is offered by driven two-level systems [17]. Specifically, we focus on dressed states emerging from closed-contour driving (CCD) of a quantum three-level system [17] [Fig. 1(a)]. These dressed states stand out due to remarkable coherence properties and tunability through the phase of the involved driving fields [17]. While dynamical decoupling by continuous driving has previously been demonstrated for electronic spins in diamond [14,17,19,26,27], STA have never been explored on such solid-state spins in their ground state [25], or on the promising three-level dressed states we study here. By combining STA and CCD, we establish an attractive, room-temperature platform for applications, e.g., in quantum sensing of high-frequency magnetic fields [28,29] on the nanoscale.

We implement these concepts on individual nitrogen-vacancy (NV) electronic spins, which, due to their room-temperature operation and well-established methods for optical spin initialization and read-out [30], provide an attractive, solid-state platform for quantum technologies. The dressed states we study emerge from the $S = 1$ electronic spin ground state of the negatively charged NV center, specifically from the eigenstates $|m_s\rangle$ of the spin projection operator \hat{S}_z along the NV axis, with $m_s = 0, \pm 1$ being the corresponding spin quantum numbers [Fig. 1(a)] [31]. To dress the NV spin states, we simultaneously and coherently drive all three available spin transitions, using microwave (MW) magnetic fields [32] to drive the $|0\rangle \leftrightarrow |\pm 1\rangle$ transitions and time-varying strain fields [26,27] to drive the magnetic dipole-forbidden $|-1\rangle \leftrightarrow |+1\rangle$ transition [Fig. 1(a) and [33]]. The resulting CCD dressed states [17] offer superior coherence

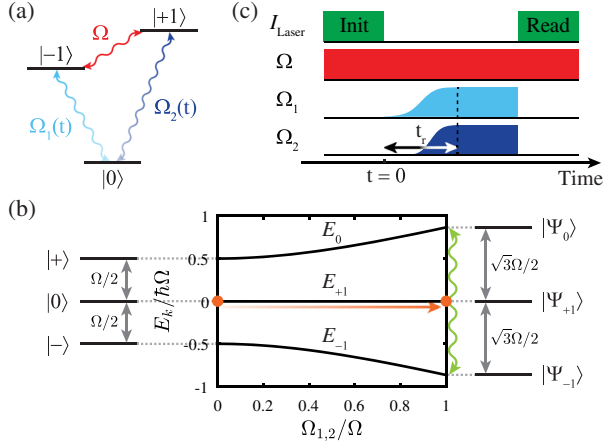


FIG. 1. State transfer schematics. (a) Level scheme of the NV $S = 1$ ground state spin with spin states $|m_s\rangle$ (magnetic quantum number $m_s = 0, \pm 1$). All three spin transitions are individually and coherently addressable, either by MW magnetic fields ($\Omega_{1,2}(t)$, light and dark blue) or by a cantilever induced strain field (Ω , red), enabling a CCD. (b) Level schemes in the rotating frame for appropriate driving field phases [see text]. The initial system (left) comprises the states $|0\rangle$ and $|\pm\rangle$, with the $|\pm\rangle$ being equal admixtures of $|\pm 1\rangle$. Ramping the amplitudes of both MW fields causes a transfer to the final dressed states $|\Psi_k\rangle$ ($k = 0, \pm 1$, right). We initialise the system in $|0\rangle$, which is for adiabatic ramping transferred to $|\Psi_{+1}\rangle$ (orange transition). (c) Pulse sequence employed for state transfer. Note that in general $\Omega_{1,2}(t)$ have different time dependencies.

protection compared to alternative approaches, which rely on MW driving alone [19]. Specifically, CCD dressed states offer decoupling from magnetic field noise up to fourth order in field amplitude [17], and for magnetometry, a more than twofold improvement in sensitivity and a 1000-fold increased sensing range [33] over previous work on dressed states [19].

The CCD dressed states are best described in an appropriate rotating frame [37] where, under resonant driving of all three transitions, the system Hamiltonian reads

$$\hat{\mathcal{H}}_0(t) = \frac{\hbar}{2} (\Omega_1(t)|-1\rangle\langle 0| + \Omega_2(t)|+1\rangle\langle 0| + \Omega e^{i\Phi}|-1\rangle\langle +1| + \text{H.c.}), \quad (1)$$

with \hbar being the reduced Planck constant. The Hamiltonian $\hat{\mathcal{H}}_0(t)$ depends on the global driving phase Φ ($\Phi = \varphi + \varphi_1 - \varphi_2$, where φ, φ_1 , and φ_2 are the phases of the driving fields with Rabi frequencies Ω , Ω_1 , and Ω_2 , respectively) [17], which we tune to $\Phi = \pi/2$. We choose this value of Φ , as it allows for a straightforward derivation of an analytical, purely real STA correction for our system. However, our method is applicable to arbitrary values of Φ using established numerical methods for determining the ensuing STA ramps [33]. For the case $\Phi = \pi/2$, the eigenstates of $\hat{\mathcal{H}}_0(t)$ prior to state transfer, i.e., for

$\Omega_{1,2}(t) = 0$ and $\Omega \neq 0$, are $|0\rangle$ and $|\pm\rangle \equiv (|-1\rangle \mp |1\rangle)/\sqrt{2}$ [Fig. 1(b), left]. In contrast, the eigenstates of the final system, i.e., for $\Omega_{1,2}(t_r) = \Omega$, are given by [17]

$$|\Psi_k\rangle = \frac{1}{\sqrt{3}} (e^{i\pi(1-4k)/6}|-1\rangle + |0\rangle + e^{-i\pi(1-4k)/6}|+1\rangle), \quad (2)$$

with $k = 0, \pm 1$ [Fig. 1(b), right]. Thus our state transfer protocol consists of spin initialization into $|0\rangle$ with $\Omega_{1,2}(t=0) = 0$, after which we apply suitable ramps $\Omega_{1,2}(t)$ to transfer into the dressed state basis with symmetric driving of all three transitions, i.e., $\Omega_{1,2}(t=t_r) = \Omega$ [Fig. 1(b)].

We study state transfer between the initial ($|0\rangle, |\pm\rangle$) and final states ($|\Psi_k\rangle$) under ambient conditions using an experimental setup described elsewhere [17] and by employing the pulse sequence shown in Fig. 1(c). A green laser pulse prepares the initial system in $|\psi(t=0)\rangle \equiv |0\rangle$. Then, we individually ramp the MW field amplitudes (with ramp time t_r) to transfer $|0\rangle$ to the dressed state $|\Psi_{+1}\rangle$ [Fig. 1(b)]. After letting the system evolve in the presence of all three driving fields, we read out the population in $|0\rangle$ at time t , $p_0(t) = |\langle 0|\psi(t)\rangle|^2$, using spin-dependent fluorescence. During the whole pulse sequence, the amplitude of the mechanical driving field is constant at $\Omega/2\pi = 510$ kHz, while the mechanical oscillator is driven near resonance at 5.868 MHz (implying $B_z = 1.82$ G).

To demonstrate state transfer into a dressed state, we first focus on an adiabatic protocol to benchmark our subsequent studies. Inspired by the ‘‘STIRAP’’ sequence developed for quantum-optical ‘‘ Λ -systems’’ [38,39], we choose [40]

$$\Omega_{1,2}(t) = \Omega \sin[\theta(t)], \quad (3)$$

[Fig. 2(a)], with

$$\theta(t) = \frac{\pi}{2} \frac{1}{1 + \exp[-\nu(t-t_0)]} \quad (4)$$

being a Fermi function with time shift $t_0 = \ln(\pi/[2\sin^{-1}(\varepsilon)] - 1)/\nu$ and free parameters ε and ν . Here, ν controls the slope of $\theta(t)$ at $t = t_0$ and is connected to the ramp time $t_r = t_0 - \ln(\pi/[2\sin^{-1}(1-\varepsilon)] - 1)/\nu$, while $\varepsilon \ll 1$ sets the amplitude of the ramp’s unavoidable discontinuities at $t = 0$ and $t = t_r$. In all our experiments we use $\varepsilon = 10^{-3}$, as this value is comparable to the estimated amplitude noise of our MW signals [33].

Figure 2(b) presents the time evolution of p_0 for several values of t_r . For fast ramping, i.e., small t_r , p_0 oscillates even for $t > t_r$; by increasing t_r , the amplitude of these oscillations reduces, until p_0 becomes time independent with $p_0 \sim 1/3$. This marks a change from a nonadiabatic to

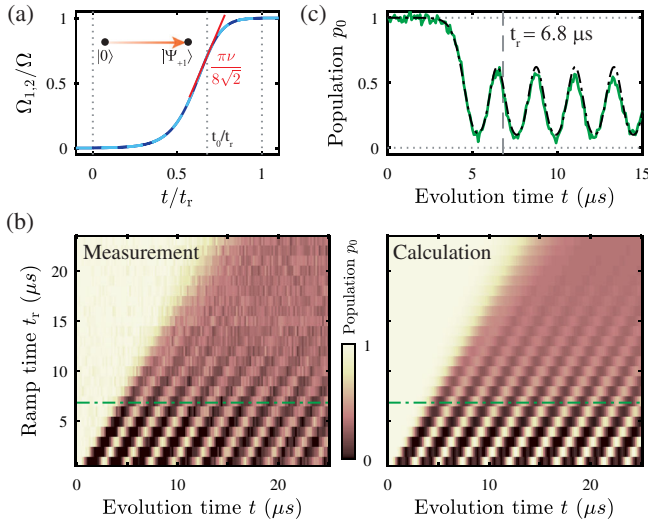


FIG. 2. Adiabatic state transfer. (a) Experimentally employed ramps for the MW field amplitudes. Both MW fields are ramped simultaneously in an optimized STIRAP pulse shape [see text]. The slope parameter ν is directly linked to the ramp time t_r . (b) Two-dimensional plots of $p_0 = |\langle 0|\psi(t)\rangle|^2$ as a function of evolution time t and ramp time t_r . The left plot shows experimental data, and the right plot shows theoretical calculations based on a fully coherent evolution. For small t_r oscillations in the population indicate a nonadiabatic transfer, whereas for slower ramping of the MW fields the state transfer becomes adiabatic. The green line indicates the location of the line cut presented in (c). (c) Line cut of measured population p_0 (green) as a function of evolution time t for $\nu = \Omega/2$ with corresponding calculation (black).

an adiabatic transition with increasing t_r [33]. Fast, non-adiabatic ramping results in a superposition of dressed states at the end of the ramp. During the subsequent time evolution each dressed state accumulates a dynamical phase, resulting in a beating (with frequency $\sqrt{3}\Omega/2$) in the measured population p_0 . Conversely, for larger t_r we adiabatically prepare the single dressed state $|\Psi_{+1}\rangle$, where no such beating occurs and $p_0 = |\langle 0|\Psi_{+1}\rangle|^2 = 1/3$, as observed in the experiment. We corroborate our experimental findings by calculating the time evolution $p_0(t)$ using Hamiltonian (1) and find excellent agreement with our data [Fig. 2(b)]. This agreement is additionally highlighted by the line cut in Fig. 2(c) taken in the nonadiabatic regime at $t_r = 6.8 \mu\text{s}$ [green dashed line indicated in Fig. 2(b)].

Having established adiabatic state transfer into the dressed state basis, we investigate STA to speed up the initialization procedure. Theoretical proposals provide various techniques for STA, including transitionless driving (TD) [21,22] or the dressed state approach to STA [41]. All techniques harness nonadiabatic transitions by adding theoretically engineered corrections to the state transfer Hamiltonian. Adding a TD control results in the correction

$$\hat{\mathcal{H}}_0(t) \rightarrow \hat{\mathcal{H}}_0(t) + i\hbar(\partial_t \hat{U}^\dagger(t))\hat{U}(t), \quad (5)$$

with $\hat{U}(t)$ being the transformation operator from $\{|m_s\rangle\}$ into the adiabatic eigenstate basis [21]. We note that in our experiment, we can only implement the TD correction of Eq. (5) for $\Phi = \pi/2$, where time reversal symmetry is maximally broken and the resulting TD correction is therefore purely real. An imaginary component would require control of the phase and amplitude of driving fields, which our mechanical-oscillator mediated strain drive cannot provide on the relevant timescales. For different values of Φ , however, other STA ramps could be found using the dressed state formalism [33,41]. Applying correction (5) to Hamiltonian (1) results in the modified MW pulse amplitudes

$$\Omega_{1,2}(t) = \Omega \sin[\theta(t)] \pm 2 \frac{\cos[\theta(t)]\partial_t\theta(t)}{2 - \cos[2\theta(t)]}, \quad (6)$$

while keeping the phases of all fields constant. Figure 3(a) shows the resulting MW pulse shapes for $\nu = \Omega/2$ and $\Omega = 510 \text{ kHz}$. Note that the TD approach provides different corrections for the two MW fields, such that both field amplitudes are ramped successively with different functional forms.

Figure 3(b) depicts the experimental result of the state transfer when applying the TD corrected ramps.

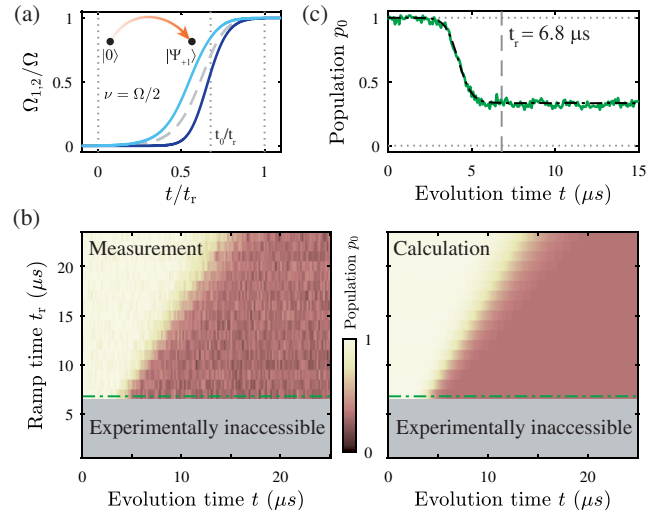


FIG. 3. STA state transfer protocol. (a) Envelope of the optimized MW field amplitudes for $\nu = \Omega/2$ and $\Omega/2\pi = 510 \text{ kHz}$. Modifications of the adiabatic pulse shape (dashed) lead to altered and unequal ramps for the two MW fields (Ω_1 light blue, Ω_2 dark blue). (b) Two-dimensional plots of p_0 as a function of evolution time t and ramp time t_r . The left plot shows experimental data, and the right plot the theoretical calculations. We achieve state transfer with high fidelity independent of t_r . The green line indicates the location of the line cut presented in (c) with ramp parameters at the experimental limit (border of grayed area). (c) Line cut of measured population p_0 (green) as function of evolution time t for the same parameters as in Fig. 2(c) with corresponding calculation (black).

Independent of t_r , the time evolution of p_0 converges to $1/3$, which indicates perfect initialization of a single dressed state, even for the fastest ramps, in striking agreement with the calculations. For TD driving, there exists a lower bound for t_r , below which the TD ramps lead to momentary driving field amplitudes either < 0 or $> \Omega$ [33]. For a fair comparison with adiabatic state transfer, we therefore exclude this parameter range from our study [grayed area in Fig. 3(b)]. The fastest possible state transfer corresponds to $\nu = \Omega/2$, resulting in $t_r = 6.8 \mu\text{s}$, the value at which the data in Fig. 3(c) have been obtained.

Figures 2(c) and 3(c) allow for a direct comparison of adiabatic and STA transfer protocols, since both measurements are recorded with the same set of experimental parameters. For the first approach, p_0 clearly indicates nonadiabatic errors in dressed state initialization [Fig. 2(c)]. However, for the TD ramp, almost no oscillations in p_0 are visible, indicating excellent state transfer [Fig. 3(c)]. The remaining small oscillations are attributed to residual imperfections in the dressed state initialization, which we discuss in the next paragraph. To achieve a transfer fidelity as determined by these residual oscillations, our calculations show that an adiabatic ramp of at least $t_r = 17.6 \mu\text{s}$ would be required, which determines the speedup factor of 2.6 we achieve for TD over adiabatic ramping for our given experimental parameters [33].

To demonstrate reversibility and to verify that the TD protocol indeed results in initialization of a single, pure dressed state, we reverse the state transfer and map from the dressed states back to the initial system. Specifically, we use the TD technique presented in Fig. 3 to prepare the system in a single dressed state, and then use an inverted TD protocol (i.e., $t \rightarrow t_r - t$) to map back to the bare NV state $|0\rangle$ [Fig. 4(a)]. Figure 4(b) shows the time evolution of p_0 as we apply the remapping protocol, where we set $\nu = \Omega/2$ (maximal ramping speed) for both directions. Clearly, almost all of the population in the dressed state returns to $|0\rangle$, thereby indicating coherent, reversible population transfer between undressed and dressed states. Additionally, such measurements allow us to quantify the efficiency of a single state transfer under the fair assumption that mapping in and mapping out yield the same transfer fidelity. We quantify the fidelity by repeatedly mapping in and out of the dressed state basis, with each set of one mapping in and one mapping out constituting a single “remapping cycle.” We vary the number of remapping cycles N and read out the population p_0 at the end [Fig. 4(c)]. An exponential fit then yields the fidelity $F = 99.4(2)\%$ for a single transfer process. This transfer fidelity is experimentally limited by uncertainties in setting the global phase Φ , leakage of the MW signals, nonequal driving field amplitudes, and unwanted detunings of the driving fields. Although we calculate our ramps assuming equal driving amplitudes and zero detunings, violations of these assumptions are experimentally unavoidable, and the

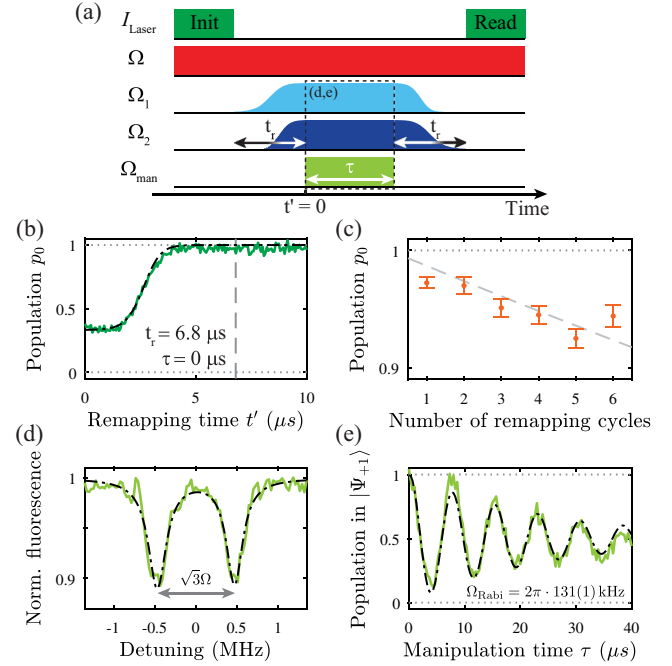


FIG. 4. Transfer fidelity and dressed state characterization. (a) Pulse sequence employed for bidirectional state transfer and manipulation of the dressed states. (b) Inverted state transfer to the initial system after the dressed state $|\Psi_{+1}\rangle$ was prepared. Measured population p_0 (green) as a function of the remapping time t' for $\nu = \Omega/2$ with corresponding simulation (black). (c) Experimental transfer fidelity for various numbers of completed (re-) mapping cycles. The exponential fit to the data (dashed) yields a statistical transfer fidelity of 99.4(2)%. (d) Transition frequencies of the dressed states after initialization of $|\Psi_{+1}\rangle$ measured with an additional probe field Ω_{man} , whose frequency is given relative to the $|0\rangle \leftrightarrow |-1\rangle$ transition of 2.8672 GHz. (e) Rabi oscillations on a dressed state transition extracted from (d) with $\Omega_{\text{Rabi}}/2\pi = 131(1)$ kHz and $T_{\text{dec}} = 24(3)$ μs .

errors generally fluctuate in time [17]. These factors are also responsible for the remaining, small oscillations in p_0 visible after state transfer in Fig. 3(c) [33].

Having shown efficient initialization of a single, pure dressed state and subsequent dressed state population read-out, we next demonstrate coherent manipulation of dressed states by performing electron spin resonance and Rabi nutation measurements in the dressed state basis. For this, we apply an additional MW manipulation field of Rabi frequency Ω_{man} in between the initialization and remapping procedures [Fig. 4(a)]. By sweeping the frequency of this manipulation field (at a constant pulse duration $\tau = 45 \mu\text{s}$) across the $|0\rangle \leftrightarrow |-1\rangle$ transition of the NV states, we observe two dips [Fig. 4(d)], corresponding to dressed state transitions at positive and negative frequencies in the rotating frame, i.e., at symmetric detunings around the bare $|0\rangle \leftrightarrow |-1\rangle$ transition frequency [note that the two possible transition from $|\Psi_{+1}\rangle$ to either $|\Psi_0\rangle$ or $|\Psi_{-1}\rangle$ [light green arrows in Fig. 1(b)] occur at the same frequencies and

are therefore indistinguishable]. Lastly, by resonant driving of the dressed state transitions for varying durations τ , we demonstrate coherent Rabi oscillations [Fig. 4(e)] and therefore coherent dressed state manipulation.

We have shown high-fidelity, reversible initialization of individual dressed states in a CCD scheme using STA state transfer protocols, for which we demonstrated a more than twofold speed-up over the adiabatic approach with state transfer fidelities $> 99\%$. This performance is the direct result of our combination of STA (providing fast, high efficiency initialization) and CCD dressed states (offering close to 100-fold improvement in coherence times compared to the other continuous mechanical or MW driving schemes under similar conditions [17]). Our results provide a basis for future exploitation of dressed states, building on the coherent control of dressed states we have demonstrated. In particular, while the efficiency of coherence protection in CCD has been demonstrated recently [17], details of additional dressed state dephasing mechanisms remain unknown and could be explored by employing noise spectroscopy [42] and dynamical decoupling [43–45], directly in the dressed state basis. Owing to the prolonged dressed state coherence times over the bare spin states [17,19,20,46], our technique could be used to efficiently store particular NV spin states by mapping to the dressed state basis [47,48] on timescales much longer than the coherence times of the bare NV states. Lastly, owing to its versatility and stability, the experimental system we established here forms an attractive platform to implement and test novel state transfer protocols, which may emerge from future theoretical work.

We thank A. Stark and J. Teissier for fruitful discussions and valuable input. We gratefully acknowledge financial support through the NCCR QSIT (Grant No. 185902), through the Swiss Nanoscience Institute, through the EU Quantum Flagship project ASTERIQS (Grant No. 820394), and through the Swiss NSF Project Grant No. 169321.

*patrick.maletinsky@unibas.ch

- [1] J. A. Jones, S. D. Karlen, J. Fitzsimons, A. Ardavan, S. C. Benjamin, G. A. D. Briggs, and J. J. L. Morton, *Science* **324**, 1166 (2009).
- [2] J. M. Taylor, P. Cappellaro, L. Childress, L. Jiang, D. Budker, P. R. Hemmer, A. Yacoby, R. Walsworth, and M. D. Lukin, *Nat. Phys.* **4**, 810 (2008).
- [3] D. Loss and D. P. DiVincenzo, *Phys. Rev. A* **57**, 120 (1998).
- [4] B. E. Kane, *Nature (London)* **393**, 133 (1998).
- [5] J. P. Home, D. Hanneke, J. D. Jost, J. M. Amini, D. Leibfried, and D. J. Wineland, *Science* **325**, 1227 (2009).
- [6] U. G. Poschinger, G. Huber, F. Ziesel, M. Deiß, M. Hettrich, S. A. Schulz, K. Singer, G. Poulsen, M. Drewsen, R. J. Hendricks, and F. Schmidt-Kaler, *J. Phys. B* **42**, 154013 (2009).
- [7] J. Clarke and F. K. Wilhelm, *Nature (London)* **453**, 1031 (2008).
- [8] R. Hanson and D. D. Awschalom, *Nature (London)* **453**, 1043 (2008).
- [9] M. A. Nielsen and I. L. Chuang, *Quantum Computation and Quantum Information* (Cambridge University Press, Cambridge, England, 2010).
- [10] L. Viola, E. Knill, and S. Lloyd, *Phys. Rev. Lett.* **82**, 2417 (1999).
- [11] G. S. Uhrig, *Phys. Rev. Lett.* **98**, 100504 (2007).
- [12] J. Du, X. Rong, N. Zhao, Y. Wang, J. Yang, and R. B. Liu, *Nature (London)* **461**, 1265 (2009).
- [13] C. M. Wilson, T. Duty, F. Persson, M. Sandberg, G. Johansson, and P. Delsing, *Phys. Rev. Lett.* **98**, 257003 (2007).
- [14] J.-M. Cai, B. Naydenov, R. Pfeiffer, L. P. McGuinness, K. D. Jahnke, F. Jelezko, M. B. Plenio, and A. Retzker, *New J. Phys.* **14**, 113023 (2012).
- [15] D. A. Golter, T. K. Baldwin, and H. Wang, *Phys. Rev. Lett.* **113**, 237601 (2014).
- [16] J. Teissier, A. Barfuss, and P. Maletinsky, *J. Opt.* **19**, 044003 (2017).
- [17] A. Barfuss, J. Kölbl, L. Thiel, J. Teissier, M. Kasparczyk, and P. Maletinsky, *Nat. Phys.* **14**, 1087 (2018).
- [18] N. Timoney, I. Baumgart, M. Johanning, A. F. Varón, M. B. Plenio, A. Retzker, and C. Wunderlich, *Nature (London)* **476**, 185 (2011).
- [19] X. Xu, Z. Wang, C. Duan, P. Huang, P. Wang, Y. Wang, N. Xu, X. Kong, F. Shi, X. Rong, and J. Du, *Phys. Rev. Lett.* **109**, 070502 (2012).
- [20] P. London, J. Scheuer, J.-M. Cai, I. Schwarz, A. Retzker, M. B. Plenio, M. Katagiri, T. Teraji, S. Koizumi, J. Isoya, R. Fischer, L. P. McGuinness, B. Naydenov, and F. Jelezko, *Phys. Rev. Lett.* **111**, 067601 (2013).
- [21] M. Demirplak and S. A. Rice, *J. Phys. Chem. A* **107**, 9937 (2003).
- [22] M. V. Berry, *J. Phys. A* **42**, 365303 (2009).
- [23] A. del Campo, *Phys. Rev. Lett.* **111**, 100502 (2013).
- [24] X. Chen, I. Lizuain, A. Ruschhaupt, D. Guéry-Odelin, and J. G. Muga, *Phys. Rev. Lett.* **105**, 123003 (2010).
- [25] B. B. Zhou, A. Baksic, H. Ribeiro, C. G. Yale, F. J. Heremans, P. C. Jerger, A. Auer, G. Burkard, A. A. Clerk, and D. D. Awschalom, *Nat. Phys.* **13**, 330 (2017).
- [26] E. R. MacQuarrie, T. A. Gosavi, A. M. Moehle, N. R. Jungwirth, S. A. Bhawe, and G. D. Fuchs, *Optica* **2**, 233 (2015).
- [27] A. Barfuss, J. Teissier, E. Neu, A. Nunnenkamp, and P. Maletinsky, *Nat. Phys.* **11**, 820 (2015).
- [28] T. Joas, A. Waeber, G. G. Braunbeck, and F. Reinhard, *Nat. Commun.* **8**, 964 (2017).
- [29] A. Stark, N. Aharon, T. Unden, D. Louzon, A. Huck, A. Retzker, U. L. Andersen, and F. Jelezko, *Nat. Commun.* **8**, 1105 (2017).
- [30] A. Gruber, A. Dräbenstedt, C. Tietz, L. Fleury, J. Wrachtrup, and C. v. Borczyskowski, *Science* **276**, 2012 (1997).
- [31] M. W. Doherty, N. B. Manson, P. Delaney, F. Jelezko, J. Wrachtrup, and L. C. Hollenberg, *Phys. Rep.* **528**, 1 (2013).
- [32] F. Jelezko, T. Gaebel, I. Popa, A. Gruber, and J. Wrachtrup, *Phys. Rev. Lett.* **92**, 076401 (2004).

- [33] See Supplemental Material at <http://link.aps.org/supplemental/10.1103/PhysRevLett.122.090502> for additional experimental and theoretical details, which includes Refs. [30,34–36].
- [34] P. Jamonneau, M. Lesik, J. P. Tetienne, I. Alvizu, L. Mayer, A. Dréau, S. Kosen, J.-F. Roch, S. Pezzagna, J. Meijer, T. Teraji, Y. Kubo, P. Bertet, J. R. Maze, and V. Jacques, *Phys. Rev. B* **93**, 024305 (2016).
- [35] A. Z. Chaudhry, *Phys. Rev. A* **90**, 042104 (2014).
- [36] C. L. Degen, F. Reinhard, and P. Cappellaro, *Rev. Mod. Phys.* **89**, 035002 (2017).
- [37] S. J. Buckle, S. M. Barnett, P. L. Knight, M. A. Lauder, and D. T. Pegg, *Opt. Acta* **33**, 1129 (1986).
- [38] K. Bergmann, H. Theuer, and B. W. Shore, *Rev. Mod. Phys.* **70**, 1003 (1998).
- [39] N. V. Vitanov, A. A. Rangelov, B. W. Shore, and K. Bergmann, *Rev. Mod. Phys.* **89**, 015006 (2017).
- [40] G. S. Vasilev, A. Kuhn, and N. V. Vitanov, *Phys. Rev. A* **80**, 013417 (2009).
- [41] A. Baksic, H. Ribeiro, and A. A. Clerk, *Phys. Rev. Lett.* **116**, 230503 (2016).
- [42] N. Bar-Gill, L. Pham, C. Belthangady, D. Le Sage, P. Cappellaro, J. Maze, M. Lukin, A. Yacoby, and R. Walsworth, *Nat. Commun.* **3**, 858 (2012).
- [43] C. A. Ryan, J. S. Hodges, and D. G. Cory, *Phys. Rev. Lett.* **105**, 200402 (2010).
- [44] G. de Lange, Z. H. Wang, D. Ristè, V. V. Dobrovitski, and R. Hanson, *Science* **330**, 60 (2010).
- [45] B. Naydenov, F. Dolde, L. T. Hall, C. Shin, H. Fedder, L. C. L. Hollenberg, F. Jelezko, and J. Wrachtrup, *Phys. Rev. B* **83**, 081201 (2011).
- [46] E. R. MacQuarrie, T. A. Gosavi, S. A. Bhave, and G. D. Fuchs, *Phys. Rev. B* **92**, 224419 (2015).
- [47] C. Simon *et al.*, *Eur. Phys. J. D* **58**, 1 (2010).
- [48] H. P. Specht, C. Nölleke, A. Reiserer, M. Uphoff, E. Figueroa, S. Ritter, and G. Rempe, *Nature (London)* **473**, 190 (2011).